International Journal of Advanced Chemistry, 6 (1) (2018) 121-131

International Journal of Advanced Chemistry

Website: www.sciencepubco.com/index.php/IJAC
doi: 10.14419/ijac.v6i1.11795
Research paper

Quantum chemical investigation of spectroscopic, electronic and NLO properties of (1E, 4E)-1-(3-nitrophenyl)-5-phenylpenta-1,4-dien-3-one

N. Benhalima [1], S. Yahiaoui [1], N. Boubegra [1], M. Boulakoud [1], Y. Megrouss [1], A. Chouaih [1] *, F. Hamzaoui [2]

[1] LTPS Laboratory, Abdelhamid Ibn Badis University of Mostaganem, 27000 Mostaganem, Algeria
[2] LPFM Académie de Montpellier – France
**Corresponding author E-mail: achouaih@gmail.com*

Abstract

In the present work the optimized molecular geometry and harmonic vibrational frequencies of chalcone derivative were calculated by DFT/B3LYP method with 6–31G (d,p) basis set. The vibrational assignments were performed on the basis of the potential energy dis-tribution (PED) of the vibrational modes. Natural bond orbital (NBO) analysis has been performed on title compound using B3LYP/6–31G (d,p) and HSEh1PBE /6–31G (d,p) levels in order to elucidate intermolecular hydrogen bonding, intermolecular charge transfer (ICT) and delocalization of electron density. Mulliken atomic charges, natural population analysis (NPA) and atomic polar tensors (APT) were performed. The nonlinear optical properties of the title compound are also calculated and discussed. Molecular electrostatic poten-tial and HOMO-LUMO energy levels are also computed. Ultraviolet–visible spectrum of the title compound has been calculated using TD–DFT method. The molecular orbital contributions were studied by density of states (DOSs). Global reactivity descriptors have been calculated using the HOMO and LUMO to predict compound reactivity.

Keywords: *DFT; HOMO; LUMO; NBO; NLO; NPA.*

1. Introduction

In recent times, chalcone derivatives have received great attention due to their anti–infective, especially antifungal and antibacterial activities (Zangade et al. 2010, Abonia et al. 2012, Tala-Tapeh et al. 2015). It has reported that the potential biological activities of chalcones, such as, anti–inflammatory (Ballesteros et al. 1995, Won et al. 2005), antitumor (Kumar et al. 2003), antimalarial (Domínguez et al. 2005, Awasthi et al. 2009), inhibition of key enzymes (Rao et al. 2009), cytotoxicity (Reddy et al. 2012), antiplatelet (Zhao et al. 2005), antileishmanial (Aponte et al. 2010), antiviral (Biradar et al. 2010), inhibitor of colon cancer cell growth (Mizuno et al. 2010), Radical-scavenging (Nabi et al. 2011), antidyslipidemic (Shukla et al. 2011), antidiabetic agents (Hsieh et al. 2012), vasorelaxant (Dong et al. 2010), antiprotozoal (Hayat et al. 2011) etc. In recent years, chalcones have been used in the field of material science as nonlinear optical (Shettigar et al. 2008, Asiri et al. 2014), optical limiting (Shettigar et al. 2006), electrochemical sensing (Delavaux-Nicot et al. 2007) and langmuir film (Gasull et al. 2002). Various materials containing chalcone moiety are notable for their second harmonic generation (Goto et al. 1991). The structure of the title compound was studied by the help of density functional theory (DFT) with B3LYP and HSEh1PBE functionals and 6-31G (d, p) basis set. The vibrational assignments have been performed based on potential energy distribution (PED). We have also performed natural bond orbital (NBO) calculation to provide a convenient basis for investigating charge transfer or conjugative interaction in molecular systems. Molecular electrostatic potential (MEP) surface and HOMO-LUMO orbitals of the title compound have been investigated by using B3LYP and HSEh1PBE levels of density functional theory (DFT) with 6–31G (d,p) as basis set. In order to show the nonlinear optic (NLO) activity of title compound, the dipole moment, linear polarizability and first hyperpolarizability were obtained. Mulliken atomic charge, natural population analysis (NPA) and atomic polar tensors (APT) were computed by DFT method. The global reactivity descriptors, namely, hardness, softness, chemical potential and electrophilicity index are also calculated to understand the reactive nature of the compound.

2. Computational details

All theoretical calculations were carried out with help of Gaussian 09 program package (Frisch et al. 2009) using B3LYP (Becke's three parameter hybrid functional with the LYP correlation functional) (Lee et al. 1988, Becke et al. 1993) and HSEh1PBE (the recommended version of the full Heyd-Scuseria-Ernzerhof functional, referred to as HSE06 in literature) (Heyd et al. 2004, Heyd et al. 2004) methods in conjunction with 6–31G(d, p) basis set. The molecular structure, MEP surfaces and HOMO-LUMO levels were visualized with the help of Gauss View program (Frisch et al. 2009). The theoretical vibrational spectra of the title compound were interpreted by means of PED using the VEDA 4 program (Jamroz et al. 2004). The calculated wavenumbers were scaled with scaling factor of 0.946 for B3LYP and 0.941 for HSEh1PBE. Natural bond orbital (NBO) calculations were performed using NBO 3.1 program (Glendening et al. 1998) as implemented in the Gaussian 09 package at the DFT/B3LYP and DFT/HSEh1PBE levels. The second order Fock−matrix was carried out to evaluate the donor (i) and acceptor (j) interaction in the NBO basis (Foster et al. 1980, Reed et al. 1983, Reed et al. 1985, Reed et al. 1985, Reed et al. 1988, Szafran et al. 2007, Sebastian et al. 2010, Tamer et al. 2015, Altürk et al. 2015). For each donor (i) and acceptor (j), the stabilization energy E $^{(2)}$ associated as:

$$E^{(2)} = q_i \frac{F(i,j)^2}{\varepsilon_i - \varepsilon_j} \tag{1}$$

The larger the $E^{(2)}$ value, the more intensive is the interaction between electron donor and electron acceptor, i.e. a more donating tendency from electron donors to acceptors and a greater extent of conjugation of the whole system. Ultraviolet–visible spectrum, excitation energies, absorbance and oscillator strengths for the title compound were obtained in the framework of TD–DFT (Cancès et al. 1997, Stratmann et al. 1998) calculations using B3LYP/6–31G (d,p) and HSEh1PBE/6–31G (d,p) functionals. Density of state (DOS) diagram of the title compound derived using the GaussSum 2.2 program (O'Boyle et al. 2008) was used to calculate group contributions to the molecular orbitals. Molecular electrostatic potential (MEP) surfaces have been investigated by using B3LYP and HSEh1PBE levels of DFT method with 6–31G (d, p) basis set. Mulliken atomic charges, natural population analysis (NPA) and atomic polar tensors (APT) (Ferreira 1993) were calculated by determining the electron population of each atom. To study the nonlinear optical properties (NLO), parameters such as dipole moment (μ), polarizability (α) and the first–order hyperpolarizability(β) are determined using B3LYP and HSEh1PBE functionals with 6–31G(d,p) basis sets. The total dipole moments (μ), polarizability (α) and first–order hyperpolarizability (β) are evaluated using the following equations:

$$\mu = \left(\mu_x^2 + \mu_y^2 + \mu_z^2\right)^{1/2} \tag{2}$$

$$\alpha = \frac{1}{3}\left(\alpha_x + \alpha_y + \alpha_z\right) \tag{3}$$

$$\beta_{tot} = \left(\beta_x^2 + \beta_y^2 + \beta_z^2\right)^{1/2} \tag{4}$$

The complete equation for calculating the magnitude of first–order hyper polarizability from Gaussian 09 output is given as follows:

$$\beta_{tot} = \left[\left(\beta_{xxx}^2 + \beta_{xyy}^2 + \beta_{xzz}^2\right)^2 + \left(\beta_{xxy}^2 + \beta_{yyy}^2 + \beta_{yzz}^2\right)^2 + \left(\beta_{xxz}^2 + \beta_{yyz}^2 + \beta_{zzz}^2\right)^2\right]^{1/2} \tag{5}$$

The α_{tot} and β_{tot} values of Gaussian output are in atomic units (a.u.) therefore they were converted into electrostatic units (esu) (for α; 1 a.u. = 0.1482 × 10^{-24}esu, for β; 1 a.u. = 8.6393 × 10^{-33}esu). The chemical reactivity descriptors of compounds such as electronegativity (χ), chemical potential (μ), hardness (η), softness (S), and electrophilicity index (ω) are evaluated using following equations (Parr et al. 1978, Parr et al. 1983, Parr et al. 1999, Chattaraj et al. 2003, Pearson 2005):

$$\chi = \frac{I + A}{2} \tag{6}$$

$$\mu = -\frac{I + A}{2} \tag{7}$$

$$\eta = \frac{I - A}{2} \tag{8}$$

$$S = \frac{1}{2}\eta \tag{9}$$

$$\omega = \frac{\mu^2}{2\eta} \tag{10}$$

3. Results and discussion

3.1. Optimized structure and hydrogen bonding

The bond lengths, bond angles and dihedral angles corresponding to the optimized geometry of the title compound have been obtained using the DFT/B3LYP/6–31(d,p) and DFT/HSEh1PBE /6–31(d,p) methods and the corresponding results are reported in Table 1. The optimized geometry of the title compound is illustrated in Fig. 1. The benzene C–C bond lengths observed in the region of 1.378–1.399 Å (Samshuddin et al. 2012) have been calculated at the range of 1.390–1.410 Å for B3LYP level and 1.386–1.406Å for HSEh1PBE level. The C7=C8 and C10=C11 bond lengths are observed as 1.332, 1.333 Å (Samshuddin et al. 2012). In our calculations, these bond length are found to be 1.346 , 1.346 Å for B3LYP level and 1.343, 1.346 Å for HSEh1PBE level. For the title compound, the C=O bond lengths (B3LYP /XRD) are 1.2308/1.2287Å which are in agreement with reported values (Samshuddin et al. 2012). The bond length between C and N is 0,001 Å times higher than the experimental value(1.465 Å). The bond length of O–N is differed from 0.003 Å to 0.01 Å with experimental value (1.2270 and 1.2202Å). The average ON distance of 1.2301Å in the nitro group is an indication of clearly double bonds. The bond angle O1–N1–O2 (124.78°) of nitro group which is closer to experimental data (123.25°). The calculated O1–N1–C3 and O2–N1–C3 angles are 117.68 and 117.54, respectively, about 0.7° smaller than the experimental results. The N1–C3–C2 and N1–C3–C4 bond angles observed as 118.73° and 118.61° (Samshuddin et al. 2012) have been also calculated as 118.79 and 118.83 for B3LYP, 118.75 and 118.80 for HSEh1PBE levels. From Table 1, it can be noted that there is a good agreement between the experimental and theoretical geometric parameters.

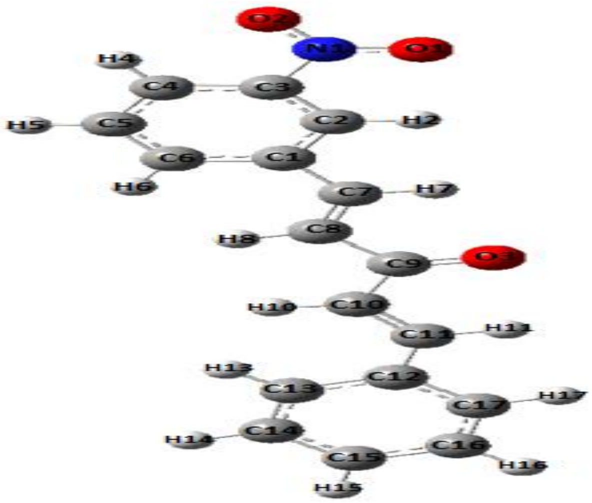

Fig. 1: The Optimized Structure of the Title Compound.

3.2. Natural bond orbital analysis

The natural bond orbital analysis have been performed by using B3LYP and HSEh1PBE methods with 6–31G (d, p) basis set. The perturbation energies of significant donor–acceptor interactions from the NBO analysis were summarized in Table 2. As concluded from the calculated NBO results, the strongest stabilization energies within title compound are defined as π (C7–C8) → π* (C9–O3) with the energies of 19.32 and 18.84 kcal/mol at B3LYP and HSEh1PBE levels, respectively. The important intramolecular hyper–conjugative interactions are: n2 (O1) →σ* (C3–N1), n2 (O1) →σ* (N1–O2), n2 (O2) →σ* (C3–N1), n2 (O2) →σ* (N1–O1), n3 (O2)→ (N1–O1) , n2 (O3)→σ* (C8–C9), n2 (O3)→σ* (C9–C10)with stabilization energies 12.84,19.30, 12.77, 19.22, 164.16, 19.79, 19.17 kJ/mol at B3LYP . The corresponding electron density values are 1.89710e, 1.89771e, 1.44242e and

1.88050e. The magnitude of charge transfer from the lone pairs of n3 (O2) to anti–bonding (N1–O1), π orbitals amount to stabilization of 164.16kcal/mol. The highly probable transition in this compound are (C1–C2) to (C3–C4) (π–π*, 20.56 kcal/mol), (C1–C2) to (C5–C6) (π→π*, 20.01 kcal/mol), (C3–C4) to (C1–C2) (π→π*, 21.60 kcal/mol), (C3–C4) to (C5–C6)(π→π*,16.48 kcal/mol), (C5–C6) to (C1–C2) (π→π*, 18.23 kcal/mol), (C5–C6) to (C3–C4) (π→π*, 22.60 kcal/mol) , these six transitions correspond to three pairs of orbitals within the first aromatic ring. $E^{(2)}$ means energy of hyperconjugative interactions (stabilization energy).

[An] Energy difference between donor and acceptor i and j NBO orbitals.

[B] F (i, j) is the Fock matrix element between i and j NBO orbitals.

Table 1: The Calculated Geometric Parameters of the Title Compound

Bond lengths (Å)	X-ray	DFT	Bond angles (°)	X-ray	DFT	Dihedral angles (°)	X-ray	DFT
O1–N1	1.227	1.229	O1–N1–O2	123.25	124.78	O1–N1–C3–C2	6.3	0.0
O2–N1	1.220	1.230	O1–N1–C3	118.38	117.68	O1–N1–C3–C4	–172.4	–179.9
O3–C9	1.228	1.230	O2–N1–C3	118.36	117.54	O2–N1–C3–C2	–173.8	–179.9
N1–C3	1.465	1.475	C2–C1–C6	118.32	118.12	O2–N1–C3–C4	7.4	0.0
C1–C2	1.394	1.404	C2–C1–C7	118.78	118.43	C6–C1–C2–C3	–1.6	–0.0
C1–C6	1.399	1.410	C6–C1–C7	122.89	123.45	C7–C1–C2–C3	177.6	180.0
C1–C7	1.467	1.464	C1–C2–C3	119.22	119.69	C2–C1–C6–C5	0.6	0.0
C2–C3	1.384	1.390	N1–C3–C2	118.73	118.79	C7–C1–C6–C5	–178.6	–180.0
C3–C4	1.383	1.392	N1–C3–C4	118.61	118.83	C2–C1–C7–C8	–173.2	–179.9
C4–C5	1.385	1.395	C2–C3–C4	122.65	122.37	C6–C1–C7–C8	6.1	0.0
C5–C6	1.383	1.392	C3–C4–C5	118.09	118.06	C1–C2–C3–N1	–177.1	–180.0
C7–C8	1.332	1.346	C4–C5–C6	120.27	120.54	C1–C2–C3–C4	1.5	0.0
C8–C9	1.482	1.489	C1–C6–C5	121.43	121.22	N1–C3–C4–C5	178.4	–180.0
C9–C10	1.479	1.481	C1–C7–C8	126.52	127.86	C2–C3–C4–C5	–0.2	–0.0
C10–C11	1.333	1.346	C7–C8–C9	122.11	120.49	C3–C4–C5–C6	–0.8	0.0
C11–C12	1.468	1.461	O3–C9–C8	122.43	121.46	C1–C7–C8–C9	–177.4	180.0
C12–C13	1.395	1.409	O3–C9–C10	122.50	122.34	C7–C8–C9–O3	–11.3	0.0
C12–C17	1.397	1.407	C8–C9–C10	115.02	116.19	C7–C8–C9–C10	166.1	–180.0
C13–C14	1.387	1.409	C9–C10–C11	121.79	120.56	O3–C9–C10–C11	21.9	0.0
C14–C15	1.386	1.399	C10–C11–C12	126.80	128.29	C8–C9–C10–C11	–155.4	–180.0
C15–C16	1.378	1.395	C11–C12–C13	122.53	123.34	C9–C10–C11–C12	176.1	180.
C16–C17	1.389	1.393	C11–C12–C17	118.99	118.49	C10–C11–C12–C13	10.4	0.0
			C13–C12–C17	118.46	118.18	C10–C11–C12–C17	–170.9	–180.0
			C12–C13–C14	120.55	120.73	C11–C12–C13–C14	178.3	–180.0
			C13–C14–C15	120.36	120.31	C17–C12–C13–C14	–0.3	0.0
			C14–C15–C16	119.65	119.74	C11–C12–C17–C16	–177.9	180.0
			C15–C16–C17	120.37	119.94	C13–C12–C17–C16	0.8	–0.0
			C12–C17–C16	120.61	121.10	C12–C13–C14–C15	–0.3	–0.0
						C13–C14–C15–C16	0.4	0.0
						C14–C15–C16–C17	0.0	–0.0

Table.2: Second–Order Perturbation Theory Analysis of Flock Matrix in NBO Basis Corresponding to the Intra–Molecular Bonds of the Title Compound.

Donor (i)	ED (i) (e)	Acceptor (j)	ED (j) (e)	$E^{(2)}$ (kcal mol^{1})	ε_j ε_i^a (a.u.)	F(i,j)^b (a.u)
π (C1–C2)	1.60465	π* (C3–C4)	0.37340	20.56	0.27	0.067
π (C1–C2)		π* (C5–C6)	0.28810	20.01	0.28	0.069
π (C1–C2)		π* (C7–C8)	0.09427	15.49	0.30	0.066
π (C3–C4)	1.64122	π* (C1–C2)	0.34153	21.60	0.30	0.072
π (C3–C4)		π* (C5–C6)	0.28810	16.48	0.29	0.063
π (C3–C4)		π* (N1–O1)	0.62218	27.22	0.15	0.061
π (C5–C6)	1.65472	π* (C1–C2)	0.34153	18.23	0.29	0.064
π (C5–C6)		π* (C3–C4)	0.37340	22.60	0.28	0.071
π (C7–C8)	1.84165	π* (C1–C2)	0.34153	12.29	0.29	0.056
π (C7–C8)		π* (C9–O3)	0.23046	19.32	0.30	0.069
π (C10–C11)	1.83189	π* (C9–O3)	0.23046	21.62	0.29	0.072
π (C10–C11)		π* (C12–C17)	0.37438	11.59	0.30	0.055
π (C12–C17)	1.61495	π* (C10–C11)	0.10872	17.10	0.29	0.068
π (C12–C17)		π* (C13–C14)	0.29620	19.18	0.28	0.067
π (C12–C17)		π* (C15–C16)	0.32266	19.60	0.28	0.067
π (C13–C14)	1.67848	π* (C12–C17)	0.37438	18.85	0.28	0.066
π (C13–C14)		π* (C15–C16)	0.32266	20.22	0.28	0.068
π (C15–C16)	1.65023	π* (C12–C17)	0.37438	21.18	0.28	0.069
π (C15–C16)		π* (C13–C14)	0.29620	18.97	0.28	0.066
π (N1–O1)	1.98600	n3 (O2)	1.44242	12.35	0.18	0.078
n2(O1)	1.89710	σ* (C3–N1)	0.10609	12.84	0.57	0.076
n2 (O1)		σ* (N1–O2)	0.05664	19.30	0.71	0.105
n2 (O2)	1.89771	σ* (C3–N1)	0.10609	12.77	0.57	0.076
n2 (O2)		σ* (N1–O1)	0.05650	19.22	0.71	0.105
n3 (O2)	1.44242	π* (N1–O1)	0.62218	164.16	0.14	0.139
n2 (O3)	1.88050	σ* (C8–C9)	0.06002	19.79	0.69	0.106
n2 (O3)		σ* (C9–C10)	0.05765	19.17	0.70	0.105
π* (C1–C2)	0.34153	π* (C7–C8)	0.09427	47.80	0.02	0.064
π* (C9–O3)	0.23046	π* (C7–C8)	0.09427	67.07	0.02	0.072
π*C9–O3)		π* (C10–C11)	0.10872	53.10	0.02	0.072
π* (C12–C17)	0.37438	π* (C10–C11)	0.10872	107.46	0.01	0.067
π* (N1–O1)	0.62218	π* (C3–C4)	0.37340	15.69	0.14	0.059

Table 3: Selected NBO Results Showing Formation of Lewis and Non– Lewis Orbitals of the Title Compound Using B3LYP/631G (D, P) Level of Theory

Bond (AB)	ED/energy(a.u.)	EDA (%)	EDB (%)	NBO	S (%)	p (%)
Σ(C1–C2)	1.97144	50.65	49.35	0.7117 (sp$^{2.01}$) C+0.7025 (sp$^{1.00}$) C	33.26 35.41	66.70 64.55
Σ(C1–C6)	1.97586	51.04	48.96	0.7144 (sp$^{1.95}$) C+0.6997 (sp$^{1.88}$) C	33.87 34.73	66.09 65.23
Σ(C1–C7)	1.97679	51.52	48.48	0.7178 (sp$^{2.05}$) C+0.6963 (sp$^{1.96}$) C	32.82 33.75	67.14 66.20
Σ(C2–C3)	1.97644	49.06	50.94	0.7004 (sp $^{1.94}$) C+0.7137 (sp $^{1.64}$) C	34.05 37.90	65.90 62.07
Σ(C3–C4)	1.97665	51.15	48.85	0.7152 (sp $^{1.65}$) C+0.6989 (sp $^{1.97}$) C	37.77 33.61	62.19 66.34
Σ(C3–N1)	1.98966	37.82	62.18	0.6150 (sp $^{3.12}$) C+0.7885 (sp $^{1.77}$) N	24.26 36.08	75.61 63.88
Σ(C4–C5)	1.97626	50.37	49.63	0.7097 (sp $^{1.83}$) C+0.7045 (sp $^{1.88}$) C	35.38 34.76	64.59 65.20
Σ(C5–C6)	1.98121	49.84	50.16	0.7060 (sp $^{1.83}$) C+0.7082 (sp $^{1.80}$) C	35.27 35.70	64.69 64.27
Σ(C7–C8)	1.98316	50.33	49.67	0.7094 (sp $^{1.64}$) C+0.7048 (sp $^{1.65}$) C	37.86 37.79	62.11 62.18
Σ(C8–C9)	1.98075	51.60	48.40	0.7183 (sp $^{2.08}$) C+0.6957 (sp $^{1.91}$) C	32.41 34.38	67.54 65.57
Σ(C9–C10)	1.98122	48.72	51.28	0.6980 (sp $^{1.84}$) C+0.7161 (sp $^{2.08}$) C	35.24 32.43	64.71 67.53
Σ(C9–O3)	1.99534	34.66	65.34	0.5888 (sp $^{2.30}$) C+0.8083 (sp $^{1.39}$) O	30.30 41.76	69.59 57.91
Σ(C10–C11)	1.98305	49.79	50.21	0.7056 (sp $^{1.65}$) C+0.7086 (sp $^{1.65}$) C	37.73 37.69	62.23 62.27
Σ(C11–C12)	1.97734	48.94	51.06	0.6995 (sp $^{1.92}$) C+0.7146 (sp $^{2.08}$) C	34.29 32.42	65.67 67.54
Σ(C12–C13)	1.97486	51.08	48.92	0.7147 (sp $^{1.94}$) C+0.6994 (sp $^{1.88}$) C	33.97 34.71	65.99 65.25
Σ(C12–C17)	1.97555	51.17	48.83	0.7153 (sp $^{1.98}$) C+0.6988 (sp $^{1.86}$) C	33.57 34.91	66.40 65.05
Σ(C13–C14)	1.98056	50.21	49.79	0.7086 (sp $^{1.79}$) C+0.7056 (sp $^{1.83}$) C	35.81 35.30	64.15 64.66
Σ(C14–C15)	1.98102	50.08	49.92	0.7076 (sp $^{1.85}$) C+0.7066 (sp $^{1.86}$) C	35.01 35.01	64.95 64.95
Σ(C15–C16)	1.98107	49.96	50.04	0.7068 (sp $^{1.84}$) C+0.7074 (sp $^{1.85}$) C	35.19 35.06	64.77 64.90
Σ(C16–C17)	1.98083	49.84	50.16	0.7059 (sp $^{1.84}$) C+0.7083 (sp $^{1.81}$) C	35.15 35.62	64.81 64.34
Σ(N1–O1)	1.99579	48.58	51.42	0.6970 (sp $^{2.13}$) N+0.7171 (sp $^{2.97}$) O	31.92 25.14	67.98 74.71
Σ(N1–O2)	1.99578	48.58	51.42	0.6970 (sp $^{2.13}$) N+0.7171 (sp $^{2.98}$) O	31.89 25.12	68.01 74.74
Π(C1–C2)	1.60465	52.47	47.53	0.7244 (sp $^{1.00}$) C+ 0.6894 (sp $^{1.00}$) C	0.00 0.00	99.97 99.95
Π(C3–C4)	1.64122	54.84	45.16	0.7405 (sp $^{1.00}$) C+ 0.6720 (sp $^{1.00}$) C	0.00 0.00	99.99 99.95
Π(C5–C6)	1.65472	51.48	48.52	0.7175 (sp $^{1.00}$) C+ 0.6965 (sp $^{1.00}$) C	0.00 0.00	99.96 99.96
Π(C7–C8)	1.84165	46.94	53.06	0.6851 (sp $^{1.00}$) C+ 0.7284 (sp $^{1.00}$) C	0.00 0.00	99.94 99.96
Π(C9–O3)	1.96464	32.49	67.51	0.5700 (sp $^{1.00}$) C+ 0.8217 (sp $^{1.00}$) O	0.00 0.00	99.85 99.70
Π(C10–C11)	1.83189	54.56	45.44	0.7386 (sp $^{1.00}$) C+ 0.6741 (sp $^{1.00}$) C	0.00 0.00	99.96 99.94
Π(C12–C17)	1.61495	51.56	48.44	0.7180 (sp $^{1.00}$) C+ 0.6960 (sp $^{1.00}$) C	0.00 0.00	99.98 99.96
Π(C13–C14)	1.67848	49.46	50.54	0.7033 (sp $^{1.00}$) C+ 0.7109 (sp $^{1.00}$) C	0.00 0.00	99.96 99.96
Π(C15–C16)	1.65023	49.43	50.57	0.7030 (sp $^{1.00}$) C+ 0.7112 (sp $^{1.00}$) C	0.00 0.00	99.96 99.96
Π(N1–O1)	1.98600	40.04	59.96	0.6327 (sp $^{1.00}$) N+ 0.7744 (sp $^{1.00}$) O	0.00 0.00	99.73 99.75
n1(O1)	1.98113			sp$^{0.34}$	74.83	25.16
n2(O1)	1.89710			sp$^{99.99}$	0.14	99.76
n1(O2)	1.98117			sp$^{0.34}$	74.86	25.14
n2(O2)	1.89771			sp$^{99.99}$	0.14	99.76
n3(O2)	1.44242			sp$^{1.00}$	0.00	99.78
n1(O3)	1.97822			sp$^{0.72}$	58.20	41.76
n2(O3)	1.88050	–	–	sp$^{1.00}$	0.00	99.80
σ*(C1–C2)	0.02070	49.35	50.65	0.7025 (sp $^{2.01}$) C – 0.7117 (sp $^{1.82}$) C	33.26 35.41	66.70 64.55
σ*(C1–C6)	0.02493	48.96	51.04	0.6997 (sp$^{1.95}$) C – 0.7144 (sp$^{1.88}$) C	33.87 34.73	66.09 65.23

Table 3: (Continued)

Bond (AB)	ED/energy(a.u.)	EDA (%)	EDB (%)	NBO	S (%)	p (%)
Σ*(C1–C7)	0.02262	48.48	51.52	0.6963 ($sp^{2.05}$) C – 0.7178 ($sp^{1.96}$) C	32.82 33.75	67.14 66.20
Σ*(C2–C3)	0.02039	50.94	49.06	0.7137 ($sp^{1.94}$) C – 0.7004 ($sp^{1.64}$) C	34.05 37.90	65.90 62.07
Σ* (C3–C4)	0.02198	48.85	51.15	0.6989 ($sp^{1.65}$) C – 0.7152 ($sp^{1.97}$) C	37.77 33.61	62.19 66.34
Σ* (C3–N1)	0.10609	62.18	37.82	0.7885 ($sp^{3.12}$) C – 0.6150 ($sp^{1.77}$) N	24.26 36.08	75.61 63.88
Σ* (C4–C5)	0.01565	49.63	50.37	0.7045 ($sp^{1.83}$) C – 0.7097 ($sp^{1.88}$) C	35.38 34.76	64.59 65.20
Σ* (C5–C6)	0.01399	50.16	49.84	0.7082 ($sp^{1.83}$) C – 0.7060 ($sp^{1.80}$) C	35.27 35.70	64.69 64.27
Σ* (C7–C8)	0.01221	49.67	50.33	0.7048 ($sp^{1.64}$) C – 0.7094 ($sp^{1.65}$) C	37.86 37.79	62.11 62.18
Σ* (C8–C9)	0.06002	48.40	51.60	0.6957 ($sp^{2.08}$) C – 0.7183 ($sp^{1.91}$) C	32.41 34.38	67.54 65.57
Σ* (C9–C10)	0.05765	51.28	48.72	0.7161 ($sp^{1.84}$) C – 0.6980 ($sp^{2.08}$) C	35.24 32.43	64.71 67.53
Σ* (C9–O3)	0.01094	65.34	34.66	0.8083 ($sp^{2.30}$) C – 0.5888 ($sp^{1.39}$) O	30.30 41.76	69.59 57.91
Σ* (C10–C11)	0.01248	50.21	49.79	0.7086 ($sp^{1.65}$) C – 0.7056 ($sp^{1.65}$) C	37.73 37.69	62.23 62.27
Σ* (C11–C12)	0.02243	51.06	48.94	0.7146 ($sp^{1.92}$) C – 0.6995 ($sp^{2.08}$) C	34.29 32.42	65.67 67.54
Σ* (C12–C13)	0.02492	48.92	51.08	0.6994 ($sp^{1.94}$) C – 0.7147 ($sp^{1.88}$) C	33.97 34.71	65.99 65.25
Σ* (C12–C17)	0.02104	48.83	51.17	0.6988 ($sp^{1.98}$) C – 0.7153 ($sp^{1.86}$) C	33.57 34.91	66.40 65.05
Σ* (C13–C14)	0.01407	49.79	50.21	0.7056 ($sp^{1.79}$) C – 0.7086 ($sp^{1.83}$) C	35.81 35.30	64.15 64.66
Σ* (C14–C15)	0.01583	49.92	50.08	0.7066 ($sp^{1.85}$) C – 0.7076 ($sp^{1.86}$) C	35.01 35.01	64.95 64.95
Σ* (C15–C16)	0.01564	50.04	49.96	0.7074 ($sp^{1.84}$) C – 0.7068 ($sp^{1.85}$) C	35.19 35.06	64.77 64.90
Σ* (C16–C17)	0.01408	50.16	49.84	0.7083 ($sp^{1.84}$) C – 0.7059 ($sp^{1.81}$) C	35.15 35.62	64.81 64.34
Σ* (N1–O1)	0.05650	51.42	48.58	0.7171 ($sp^{2.13}$) N – 0.6970 ($sp^{2.97}$) O	31.92 25.14	67.98 74.71
Σ* (N1–O2)	0.05664	51.42	48.58	0.7171 ($sp^{2.13}$) N – 0.6970 ($sp^{2.98}$) O	31.89 25.12	68.01 74.74
Π* (C1–C2)	0.34153	47.53	52.47	0.6894 ($sp^{1.00}$) C – 0.7244 ($sp^{1.00}$) C	0.00 0.00	99.97 99.95
Π* (C3–C4)	0.37340	45.16	54.84	0.6720 ($sp^{1.00}$) C – 0.7405 ($sp^{1.00}$) C	0.00 0.00	99.99 99.95
Π* (C5–C6)	0.28810	48.52	51.48	0.6965 ($sp^{1.00}$) C– 0.7175 ($sp^{1.00}$) C	0.00 0.00	99.96 99.96
Π* (C7–C8)	0.09427	53.06	46.94	0.7284 ($sp^{1.00}$) C – 0.6851 ($sp^{1.00}$) C	0.00 0.00	99.94 99.96
Π* (C9–O3)	0.23046	67.51	32.49	0.8217 ($sp^{1.00}$) C – 0.5700 ($sp^{1.00}$) O	0.00 0.00	99.85 99.70
Π* (C10–C11)	0.10872	45.44	54.56	0.6741 ($sp^{1.00}$) C – 0.7386 ($sp^{1.00}$) C	0.00 0.00	99.96 99.94
Π* (C12–C17)	0.37438	48.44	51.56	0.6960 ($sp^{1.00}$) C – 0.7180 ($sp^{1.00}$) C	0.00 0.00	99.98 99.96
Π* (C13–C14)	0.29620	50.54	49.46	0.7109 ($sp^{1.00}$) C – 0.7033 ($sp^{1.00}$) C	0.00 0.00	99.96 99.96
Π* (C15–C16)	0.32266	50.57	49.43	0.7112 ($sp^{1.00}$) C – 0.7030 ($sp^{1.00}$) C	0.00 0.00	99.96 99.96
Π* (N1–O1)	0.62218	59.96	40.04	0.7744 ($sp^{1.00}$) N – 0.6327 ($sp^{1.00}$) O	0.00 0.00	99.73 99.75

Table 4: The Molecular Electric Dipole Moment M (Debye), Polarizability A_{tot} ($\times 10^{-23}$ Esu) and First Order Hyperpolarizability B_{tot} ($\times 10^{-30}$ Esu) Values of Title Compound

Parameters	B3LYP	Parameters	B3LYP
μ_x	–5.075	β_{xxx}	–2452.638
μ_y	5.120	β_{xxy}	–1540.676
μ_z	0.000	β_{xyy}	–25.275
μ (D)	7.210	β_{yyy}	59.765
α_{xx}	454.420	β_{xxz}	–1.398
α_{xy}	–3.548	β_{xyz}	–0.173
α_{yy}	200.126	β_{yyz}	–0.443
α_{xz}	0.005	β_{xzz}	–1.200
α_{yz}	–0.001	β_{yzz}	3.105
α_{zz}	64.036	β_{zzz}	0.992
α_{tot} (a.u)	239.528	β_{tot} (a.u)	2886.158
$\alpha_{tot} \times 10^{-23}$(esu)	3.545	$\beta_{tot} \times 10^{-30}$(esu)	24.936

The intra–molecular interactions due to the orbital overlap of π (C12–C17) over π* (C13–C14) and π* (C15–C16) with energies 19.18 kcal/mol and 19.60 kcal/mol, π (C13–C14) over π* (C12–C17) and π* (C15–C16) with stabilization energies 18.85 kcal/mol and 20.22 kcal/mol and π (C15–C16) over π* (C12–C17) and π* (C13–C14) with energies 21.18 kcal/mol and 18.97 kcal/mol. these six transitions correspond to three pairs of orbitals within the second aromatic ring. Further the other high energy interactions involving the delocalization of π* electrons of aromatic with the anti–bonding π* electrons of aromatic corresponds to π* (C12–C17) →π* (C10–C11) and π* (C1–C2) / π* (C7–C8) stabilizes the compound by stabilization energy in the range of 47.80107.46kJ/mol.

The large hyperconjugative interaction energies which are presented in Table 2 display the presence of intramolecular charge transfer (ICT) in title compound . It is well known that ICT induce the nonlinear optical properties of molecular systems.

The second order perturbation energies of significant donor–acceptor interactions and occupancy of electrons and p–character in significant NBO natural atomic hybrid orbitals were presented in Table 3. Selected bond taken from Table 3, σ (C9–O3) is composed of 0.5888 ($sp^{2.30}$) C+0.8083 ($sp^{1.39}$) O. The numbers 0.5888 and 0.8083 represent the polarization co–efficient. The biggest value of the polarization coefficient, indicate higher value of the electronegativity. The weights are obtained from the squares of the coefficients as $(0.8083)^2 \approx$ 0, 65334889, corresponding to 65.34 % localization on oxygen atom. In a similar way, the 34.66 % localization on carbon is obtained. The oxygen has larger percentage of this NBO, at 65.34 % and gives the larger polarization coefficient of 0.8083 because it has higher electro negatively. In σ (C3–N1)orbital with 1.98966 electrons has 37.82 % C3character in a sp2.06 hybrid and has 36.43% C9 character in asp$^{3.12}$ hybrid. The nitrogen has larger percentage of NBO at 62.18 % and gives the larger polarization coefficient of 0.7885 becauseof its higher electro negativity.

3.3. Frontier molecular orbital analysis

The HOMOLUMO energy gap of the title compound was computed at DFT/B3LYP/6-31G (d, p) and DFT/ HSEH1PBE /6-31G (d, p) levels. The electron density plots of the HOMO and LUMO for the title compound is presented in Fig. 2. The energy band gap is 3.7567 eV from B3LYP and 3.4010 from HSEH1PBE shown in Fig. 2. The small value of band gap reflects the chemical activity of the compound and encourages the application of the title compound as nonlinear optical materials.

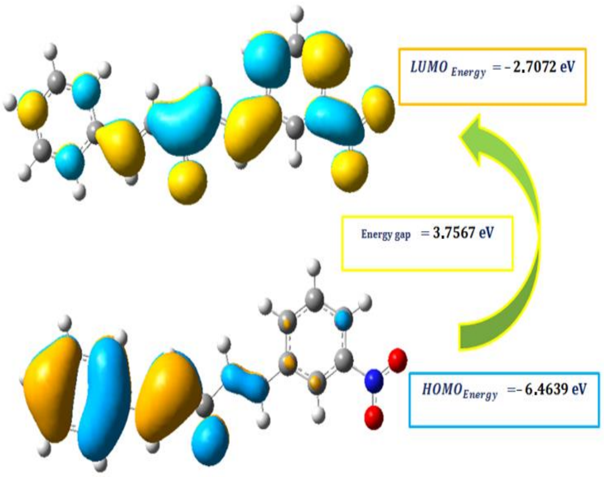

Fig. 2: The Molecular Orbitals and Energies for the HOMO and LUMO of the Title Compound.

3.4. Molecular electrostatic potential (MESP) analysis

Electrostatic potential in the MEP plot is increasing in the order of red < orange < yellow < green < blue. Electrostatic potential surface has been plotted for the title compound with B3LYP/6–31G (d,p) basis set using the computer software Gauss view as shown in Fig. 3. The negative regions are mainly localized on the nitro group and oxygen atom, a maximum positive region is localized on the hydrogen atoms indicating a possible site for nucleophilic attack.

3.5. Nonlinear optical properties

The non–linear optic properties (NLO) of the title compound was studied by calculating the dipole moment, polarizability and first order polarizability using B3LYP and HSEh1PBE methods with 6–31G (d,p) basis set. The NLO properties are summarized in Table 4.

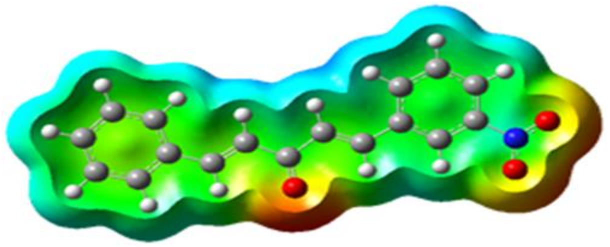

Fig. 3: Molecular Electrostatic Potential Map Obtained with B3LYP/6–31G (D, P) Level.

The calculated molecular dipole moment 7.2100 and 7.1500D for B3LYP and HSEh1PBE levels, respectively. The calculated molecular polarizability (α) values equal 35.498×10^{-23} and 35.093×10^{-23} (e.s.u) for B3LYP and HSEh1PBE levels, respectively .The first order static hyperpolarizability (β) parameter has been calculated as 24.936×10^{-30} and 23.9523×10^{-30} (e.s.u.) respectively. Our title compound with greater dipole moment and hyperpolarizability value shows that the compound has large NLO optical property.

3.6. Vibrational assignments

The title compound consists of 34 atoms, which has 96 normal modes of vibration. The vibrational band assignments were made by the aid of potential energy distribution (PED) using VEDA program. Vibrational frequency assignments of the title compound are reported in Table 5. The calculated infrared spectra of the title compound are shown in Fig. 4. Generally, the aromatic structure shows the presence of CH stretching vibration in the region 3100–3000 cm^1 (Silverstein et al. 1981, Wade 1992, Rastogi et al. 2002). In this present study, the C–H stretching vibrations are observed at 3074 to 3023 cm^{-1} [mode number 96 to 90] by B3LYP/6–31G (d,P) method. The PED corresponding to this pure mode of title compound contributed 86% to 99%. The C–C–H in plane bending vibrations are normally occurred as a number of strong to weak intensity bands in the region 1300–1000 cm^{-1}. The theoretical wave numbers for B3LYP level at 1456, 1443, 1411, 1166, 1143, 1134, 1126 and 1058cm^{-1} (mode no 75, 74, 73, 61, 60, 59, 58, 56) are assigned as C–C stretching vibrations with PED contributions of 60, 52, 46, 34, 76, 64, 79 and 21 %, respectively. The C–H out–of–plane bending vibrations are strongly coupled vibrations and occur in the region 1000–750 cm^{-1}.

The C–C stretching vibrations of aromatic compounds are expected in the range from 1650 to 1200 cm^{-1}. The theoretical wave numbers for B3LYP level at 1585,1570, 1545, 1541, 1533, 1391, 1306, 1052, 1296, 1052and 998cm^{-1} (mode no 81, 80, 78, 77, 76, 72, 65, 55, 69, 53) are assigned as C–C stretching vibrations with PED contributions of 61, 36, 69, 58, 41, 45,40,53,31 and 69 %, respectively. The C=O stretching modes are expected around 1600 to 850 cm^{-1}. The C=O stretching vibrations are computed at 1659 c N, stretching; δ, Scissoring; ρ, rooking; β, out–of–plane deformation; ω, wagging; τ, twisting; s, symmetric; as, antisymmetric. Percentage PED analysis is given in the brackets and PED contribution less than 10% is neglected.

M–1 for B3LYP level, and 1679 cm^{-1} for HSEh1PBE levels.

Table 5: Vibrational Frequency Assignments of the Title Compound.

N	N (cm^{-1}) Unscaled	N (cm^{-1}) Scaled	IR Intensities	Force constants	Assignments with PED (%)
96	3250	3074	4.9186	6.8016	νCHA(97)
95	3237	3062	3.3991	6.7387	νCHA (99)
94	3215	3041	11.3095	6.6621	νCHA (97)
93	3212	3038	23.7172	6.6746	νCHA (94)
92	3204	3030	30.7404	6.6186	νCHA (87)
91	3200	3027	4.5376	6.5594	νCHA (96)
90	3196	3023	7.1918	6.5653	νCHA (86)
89	3188	3015	3.1220	6.5121	νCH (80)
88	3184	3011	11.7789	6.5026	νCH84)
87	3182	3010	5.3043	6.4725	νCHA (89)
86	3175	3003	3.1108	6.4611	νCH (84)
85	3171	2999	0.8418	6.4612	νCH (87)
84	3165	2993	0.6841	6.4288	νCH (95)
83	1754	1659	53.7228	13.3005	νO=C (76)
82	1686	1595	404.4244	10.2698	νC=C (53) + δHC=C (16)
81	1676	1585	348.9516	11.7843	νCCA (61)
80	1660	1570	30.9754	9.9889	νC=C (19) + νCCA (36)
79	1649	1560	133.9619	10.8885	νC=C (55)
78	1634	1545	113.8118	12.424	νCCA (69)
77	1629	1541	50.0131	8.1016	νCCA (58)
76	1621	1533	26.4681	9.8053	νCCA (41) + δCCCA (11)
75	1539	1456	12.4340	3.1253	δHCCA (60)
74	1526	1443	13.8891	3.4060	δHCCA (52)
73	1492	1411	32.6404	2.9953	νCCA (28)+ δHCCA (46)
72	1471	1391	22.3459	4.0263	νCCA (45)+ δHCCA (25)
71	1400	1324	313.3061	16.0304	νasON (78) + δONO (12)
70	1381	1306	258.2036	4.3298	νCCA (40)
69	1370	1296	27.4344	4.2871	νCCA (53) + δHC=C (14)
68	1369	1295	49.0893	1.5729	δHC=C (70)
67	1355	1282	16.4706	1.5810	δHC=C (63)
66	1346	1273	8.9122	1.9745	νCC (29) + δHC=C (37)
65	1330	1258	49.1069	1.6438	ρHCCA (46)
64	1321	1249	29.8177	1.8979	νCC (10) + δHC=C (12) + ρHCCA (12)
63	1303	1232	7.3313	1.9718	νCC (23) + δHCCA (23)
62	1236	1169	5.8638	1.5994	νCCA (20) + νCC (13) + δHC=C (27) + δHCCA (10)
61	1233	1166	23.9357	1.7645	νCCA (21) + δHCCA (34)
60	1209	1143	23.5938	0.9986	νCCA (11) + δHCCA (76)
59	1199	1134	22.7958	0.9772	νCCA (10) + δHCCA (64)
58	1190	1126	1.0758	0.9180	νCCA (11) + δHCCA (79)
57	1124	1063	129.7697	1.5137	νCCA (10) + νCC (21) + δHCCA (11)
56	1119	1058	156.6727	1.3876	νCCA (11) + δHCCA (21)
55	1112	1052	13.5393	1.1504	νCCA (31) + δHCCA (27)
54	1106	1046	235.6977	1.1838	νCC (19) + δHCCA (21)
53	1055	998	1.1878	1.4524	νCCA (69) + δHCCA (14)
52	1043	986	41.0081	0.7500	ωHC=CC (76)
51	1035	979	2.9354	0.7352	ωHC=CC (78)
50	1016	961	1.1430	3.7441	νCCA (29) + δCCCA (41)
49	1015	960	7.7061	3.6329	νCCA (25) + δCCCA (39) + δCC=C (17)
48	1002	948	0.3629	0.7505	τHCCCA (71) + τCCCCA (10)
47	997	943	0.0088	0.7695	τHCCCA (63) + τCCCCA (20)
46	987	934	0.2686	2.5421	νCC (59)
45	974	921	0.0029	0.7591	τHCCCA (76) + τCCCCA (11)
44	954	902	2.7715	0.7669	τHCCCA (12) + τHCCN (70)
43	937	886	0.0054	0.7814	τHCCN (61) + τHC=CC (13)
42	936	885	24.2823	2.2872	νNC (14) + δCCCA (21)
41	934	883	0.0487	0.7263	τHCCCA (73)
40	910	861	22.8718	0.9907	τHC=CC (61) + βOCCC (12)
39	869	822	1.1823	1.8757	δCCCA (28) + δCNO (23)
38	864	817	0.3940	0.7159	τHCCC (53) + τHCCCA (16)
37	852	806	0.1326	0.5772	τHCCC (10) + τHCCCA (78)
36	834	789	32.7467	3.2672	δONO (33) + δCCCA (13)
35	823	778	15.7483	0.6467	ωHCCCA(63) + βOCON (10)
34	777	735	37.1860	0.7550	ωHCCCA (49) + τCCCCA (10)
33	757	716	1.9017	2.3553	δCNO (12) + δONO (13) + δCC=C (24)
32	748	707	9.4367	1.2658	βOCON (57)
31	717	678	36.9770	0.5752	ωHCCCA (23) + βOCCC (23)
30	696	658	2.0344	0.6677	ωHCCCA (14) + τCCCCA (34)
29	688	651	20.9396	2.1043	δCCCA (55) + δONO (12)
28	669	633	6.2325	0.8206	ωCCCCA (11) + βOCCC (25)
27	633	599	0.4296	1.5133	δCCCA (80)
26	603	570	1.0982	1.4269	νCC (10) + δCCCA (29) + δCNO (11)
25	568	537	69.6510	1.2925	δCCC (11) + δCCCA (27)
24	559	529	18.0280	1.0257	δCCCA (50)

23	528	499	2.5960	0.6748	τCCCCA (45)

Table 5: (Continued)

N	N (cm^{-1}) Unscaled	N(cm^{-1}) Scaled	IR Intensities	Force constants	Assignments with PED (%)
22	515	487	0.7856	0.8282	δCNO (66)
21	498	471	7.3447	0.4217	βCCCC (63)
20	438	414	0.0543	0.3713	βCCCC (13) + τCCCCA (54)
19	427	404	5.0972	0.6730	νNC (16) + δCCC (27)
18	413	391	0.0202	0.2922	τHCCCA (21) + τCCCCA (73)
17	379	358	6.1811	0.6139	νNC (29) + δONO (12) + δCCCA (11)
16	294	278	0.6106	0.3420	δCC=C (62)
15	288	272	1.6970	0.1522	τCCCCA (55)
14	284	269	0.0593	0.1562	τCCCCA (34) + τCC=CC (35)
13	272	257	4.2743	0.3510	δCCCA (65)
12	198	187	2.4883	0.1607	δCCC (51)
11	187	177	0.0001	0.0511	τC=CCC (77)
10	173	164	1.2501	0.0894	τCCCCA (77)
09	165	156	0.2678	0.1090	νCC (32) + δCC=C (37)
08	104	98	0.9337	0.0336	τC=CCC (49) + τCCCCA (13)
07	94	89	0.6286	0.0347	δCC=C (80)
06	83	79	0.1244	0.0198	τCCCCA (46) + τCC=CC (26)
05	71	67	0.7493	0.0104	τCCCCA (17) + τC=CCC (51)
04	48	45	0.6288	0.0179	τCCCCA (72)
03	33	31	0.1215	0.0042	δCC=C(76)
02	20	19	0.4246	0.0011	τC=CCC (11) + τCCCCA (62)
01	12	11	0.0476	0.0007	τCCCCA (80)

Table 6: Thermo Dynamical Parameters of Title Compound Calculated at B3LYP/6–31G (D, P)

Parameters	Value	Parameters	Value
μ(D)	7.21	HOMO (EV)	–6.46
I	6.46	LUMO (eV)	–2.71
A	2.71	ΔE (eV)	3.76
χ	4.59	Zero–point vibrational energy (J/Mol)	935.70
μ	4.59	Zero–point correction (hatred/particle)	0.26
η	1.88	Thermal correction to energy	0.28
S	0.94	*Thermal correction to enthalpy*	0.28
ω	5.60	Thermal correction to Gibbs free Ennery	0.21

Table 7: Calculated Absorption Wavelength Λ (Nm), Excitation Energies E (Ev) and Oscillator Strengths (F) of the Title Compound Using TD-DFT/B3LYP/6-31G (D, P) Basis Set.

Wavelength λ(nm)	361.88	333.68
Excitation energy (eV)	3.4261	3.7157
Oscillator strengths (f)	0.4519	0.2275
Major contributions	HOMO→LUMO (97%)	H–2→LUMO (13%) H–2→L+1 (27%) HOMO→L+1 (55%)
Minor contribution	H–2→LUMO (2%)	H–4→LUMO (2%)

Table 8: Atomic Charges of the Title Compound

Atoms	Mulliken	NPA	APT	Atoms	Mulliken	NPA	APT
C1	0.110	–0.075	–0.017	N1	0.391	0.514	1.237
C2	–0.131	–0.185	–0.030	O1	–0.392	–0.378	–0.650
C3	0.236	0.057	–0.100	O2	–0.393	–0.380	–0.685
C4	–0.083	–0.206	–0.057	O3	–0.500	–0.570	–0.859
C5	–0.101	–0.231	–0.078	H2	0.144	0.276	0.109
C6	–0.089	–0.178	–0.019	H4	0.141	0.276	0.105
C7	–0.082	–0.156	0.300	H5	0.108	0.253	0.027
C8	–0.146	–0.292	–0.599	H6	0.099	0.243	0.046
C9	0.408	0.493	1.527	H7	0.129	0.259	0.064
C10	–0.146	–0.316	–0.757	H8	0.081	0.222	0.027
C11	–0.090	–0.134	0.491	H10	0.079	0.222	0.026
C12	0.127	–0.089	–0.145	H11	0.122	0.253	0.057
C13	–0.108	–0.199	–0.028	H13	0.086	0.236	0.034
C14	–0.089	–0.235	–0.070	H14	0.093	0.243	0.015
C15	–0.078	–0.220	–0.022	H15	0.094	0.243	0.018
C16	–0.088	–0.236	–0.027	H16	0.095	0.245	0.013
C17	–0.124	–0.198	0.008	H17	0.097	0.243	0.037

The C=C stretching modes are expected around 1650 to 1100 cm–1 (Clothup et al. 1990, Roeges 1994) when conjugated with a carbonyl group (Socrates 1981). The carbonyl stretching vibrations appear in the region 1750–1600 cm1. In the present case, the band calculated at 1659 cm1with PED contribution of 76 % was assigned as the carbonyl stretching vibration, which are in well agreement with the reported values for chalcone derivatives (Al-wani Zainuri et al. 2017). The NO2 group compounds are readily identified by asymmetric and symmetric stretching bands. The asymmetric NO2 stretching vibrations are generally observed in the region 1570–1485 cm–1, while the symmetric stretch will appear between 1370–1320 cm–1 (Meislich et al. 1993). In the present compound, the strong band at 1400 cm−1 by DFT method has been assigned to asymmetric stretching mode of N–O.

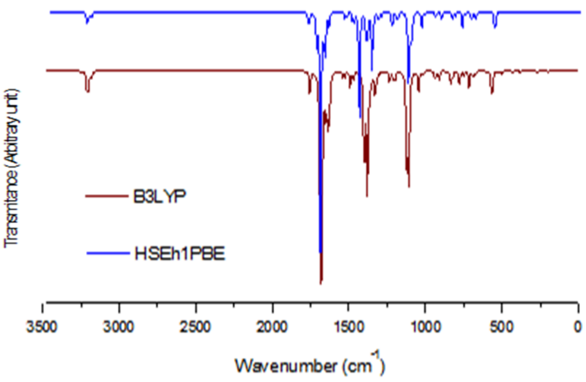

Fig. 4: The Calculated Infrared Spectra of the Title Compound.

3.7. Global reactivity descriptors and thermodynamic parameters

Energies of frontier molecular orbitals (EHOMO, ELUMO), have been used to calculate global chemical reactivity descriptors of compounds such as ionization potential , electron affinity, electronegativity, Global hardness, global softness, chemical potential and electrophilicity index. The calculated HOMO–LUMO energies, Energy gap are presented in Table 6. The Ionization potential (I) and an electron affinity (A) of the title compound calculated by B3LYP and HSEh1PBE levels are 6.4639 , 6.3551 eV and 2.7072 , 2.9543 eV respectively. The calculated values of the hardness, softness, chemical potential, electronegativity and electrophilicity index of our compound at B3LYP are 1,8784 , 0,9392 , –4,5855 , 4,5855 and 5,5973 respectively as shown in Table 6. It is seen that the chemical potential of title compound is negative which means that these substances are stable. The values of some thermodynamic parameters of the title compound calculated using B3LYP/6–and 31G (d,p) HSEH1PBE/6–31G (d,p) levels are summarized in Table 6.

3.8. Electronic properties and UV spectra

In order to recognize electronic transitions of the title compound, calculations in gas phase were performed by using TD–DFT/B3LYP/631G (d,p) for six excited states. The calculated absorption wavelengths (λ), oscillator strengths (f), and excitation energies (E) are given Table 7. The theoretical UV–Vis spectra of the title compound are shown in Fig 5. The calculated value at 361.88 nm is attributed to HOMO→LUMO electronic transition with 97% contribution . The electronic transitions is due to n →π* transition and may be attributed to the excitation of C=O group. Gauss–Sum 2.2 program was used to calculate group contributions to the molecular orbitals and prepare the density of states spectrum in Fig. 5.

3.9. Mulliken population analysis and natural population analysis

The calculated Mulliken charge values are listed in Table 8. The better represented graphical forms of our results were depicted in Fig. 6. The magnitude of the carbon atomic charge is found to be positive and negative. The magnitude of the hydrogen atomic charges is found to be only positive and is arranged in an order from 0.079012 to 0.144755 for title compound. The maximum atomic charge is obtained for C9 when compared with other atoms. This is due to the attachment of negatively charged carbon C9 atom. Negatively charged lone pair oxygen (O3) atom shows that charge is transferred from C to O (C9→O3).

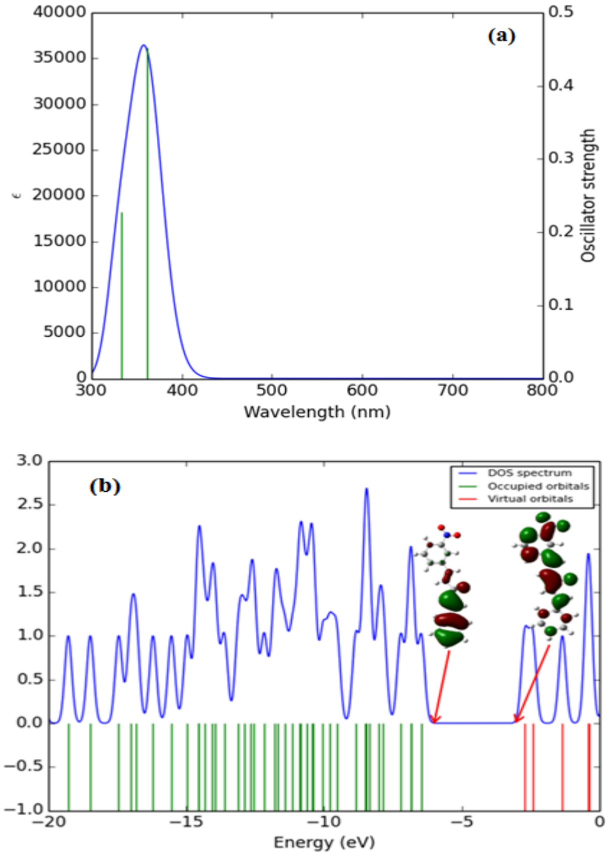

Fig. 5: Theoretical UV-Vis Spectrum (A) and Density of States (DOS) Diagram (B) of the Title Compound

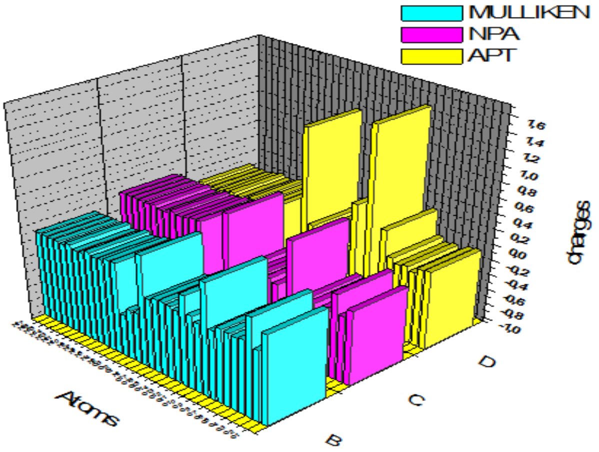

Fig. 6: The Mulliken Charges Diagram of the Title Compound.

4. Conclusion

The optimized geometrical parameters of title compound were performed and analyzed using DFT calculation based on B3LYP and HSEH1PBE levels of theory with the standard basis set 6–31G (d, p). The vibrational wavenumbers, infrared intensities and force constants were calculated and a complete vibrational analysis of the title compound has been carried out. The dipole moment, polarizability and first order hyperpolarizability of the studied compound have been calculated by DFT method which indicated that the title compound is a material which has substantial nonlinear optical character. The frontier molecular orbitals have been visualized and the HOMO–LUMO energy gap has been calculated and can be used to estimate the ionization potential, electron affinity, electronegativity, electrophilicity index, global hardness, softness and chemical potential of the compound. Finally, all these results displayed that the title compound exhibits considerable NLO properties.

References

[1] Abonia R, Insuasty D, Castillo J, Insuasty B, Quiroga J, Nogueras M & Cobo J (2012), Synthesis of novel quinoline-2-one based chalcones of potential anti-tumor activity. *European Journal of Medicinal Chemistry* 57, 29-40. https://doi.org/10.1016/j.ejmech.2012.08.039.

[2] Zangade SB, Jadhav JD, Lalpod, Vibhute YB & Dawane BS (2010), Synthesis and antimicrobial activity of some new chalcones and flavones containing substituted naphthalene moiety. *Journal of Chemical and Pharmaceutical Research* 2(1), 310-314.

[3] Tala-Tapeh SM, Mahmoodi N & Vaziri A (2015) Synthesis of bis-chalcones based on 5, 5´-methylene bis(2-hydroxybenzaldehyde) and screening their antibacterial activity. *Journal of Applied Chemistry* 9(32), 53-58.

[4] Ballesteros JF, Sanz MJ, Ubeda A, Miranda MA, Iborra S, Paya M & Alcarz MJ (1995), Synthesis and Pharmacological Evaluation of 2'-Hydroxychalcones and Flavones as Inhibitors of Inflammatory Mediators Generation. Journal of Medicinal Chemistry 38(14), 2794-2797. https://doi.org/10.1021/jm00014a032.

[5] Won SJ, Liu CT, Tsao LT, Weng JR, Ko HH, Wang JP & Lin CN (2005), Synthetic chalcones as potential anti-inflammatory and cancer chemopreventive agents. European Journal of Medicinal Chemistry 40(1), 103-112. https://doi.org/10.1016/j.ejmech.2004.09.006.

[6] Kumar SK, Hager E, Pettit C, Gurulingappa H, Davidson NE & Khan SR (2003), Design, synthesis, and evaluation of novel boronic-chalcone derivatives as antitumor agents. Journal of Medicinal Chemistry 46(14), 2813-2815. https://doi.org/10.1021/jm030213.

[7] Domínguez JN, León C, Rodrigues J, De Domínguez NG, Gut J & Rosenthal PJ (2005), Synthesis and antimalarial activity of sulfonamide chalcone derivatives. Il Farmaco 60, 307-311. https://doi.org/10.1016/j.farmac.2005.01.005.

[8] Awasthi SK, Mishra N, Kumar B, Sharma M, Bhattacharya A, Mishra LC & Bhasin VK (2009), Potent antimalarial activity of newly synthesized substituted chalcone analogs in vitro. Medicinal Chemistry Research 18(6), 407-420. https://doi.org/10.1007/s00044-008-9137-9.

[9] Rao YK, Fang SH & Tzeng YM (2009), Synthesis and biological evaluation of 3′, 4′, 5′-trimethoxychalcone analogues as inhibitors of nitric oxide production and tumor cell proliferation. Bioorganic & Medicinal Chemistry 17(23), 7909-7914. https://doi.org/10.1016/j.bmc.2009.10.022.

[10] Reddy MVB, Shen YC, Ohkoshi E, Bastow KF, Qian K, Lee KH & Wu TS (2012), Bis-chalcone analogues as potent NO production inhibitors and as cytotoxic agents. *European Journal of Medicinal Chemistry* 47, 97-103. https://doi.org/10.1016/j.ejmech.2011.10.026.

[11] Zhao LM, Jin SH, Sun LP, Piao HR & Quan ZS (2005), Synthesis and evaluation of antiplatelet activity of trihydroxychalcone derivatives. Bioorganic & Medicinal Chemistry Letters 15(22), 5027-5029. https://doi.org/10.1016/j.bmcl.2005.08.039.

[12] Aponte JC, Castillo D, Estevez Y, Gonzalez G, Arevalo J, Hammond GB & Sauvain M (2010), In vitro and in vivo anti-Leishmania activity of polysubstituted synthetic chalcones. Bioorganic & Medicinal Chemistry Letters 20(1), 100-103. https://doi.org/10.1016/j.bmcl.2009.11.033.

[13] Biradar JS, Sasidhar BS & Parveen R (2010). Synthesis, antioxidant and DNA cleavage activities of novel indole derivatives. European Journal of Medicinal Chemistry 45, 4074-4078. https://doi.org/10.1016/j.ejmech.2010.05.067.

[14] Mizuno CS, Paul S, Suh N & Rimando AM (2010), Synthesis and biological evaluation of retinoid-chalcones as inhibitors of colon cancer cell growth. Bioorganic & Medicinal Chemistry Letters 20(24), 7385-7387. https://doi.org/10.1016/j.bmcl.2010.10.038.

[15] Nabi G & Liu ZQ (2011), Radical-scavenging properties of ferrocenyl chalcones. Bioorganic & Medicinal Chemistry Letters 21(3), 944-946. https://doi.org/10.1016/j.bmcl.2010.12.051.

[16] Shukla P, Srivastava SP, Srivastava R, Rawat AK, Srivastava AK & Pratap R (2011), Synthesis and antidyslipidemic activity of chalcone fibrates. Bioorganic & Medicinal Chemistry Letters 21(11), 3475-3478. https://doi.org/10.1016/j.bmcl.2011.03.057.

[17] Hsieh CT, Hsieh TJ, El-Shazly M, Chuang DW, Tsai YH, Yen CT, Wu SF, Wu YC & Chang FR (2012), Synthesis of chalcone derivatives as potential anti-diabetic agents. Bioorganic & Medicinal Chemistry Letters 22(12), 3912-3915 https://doi.org/10.1016/j.bmcl.2012.04.108.

[18] Dong X, Du L, Pan Z, Liu T, Yang B & Hu Y (2010), Synthesis and biological evaluation of novel hybrid chalcone derivatives as vasorelaxant agents. European Journal of Medicinal Chemistry 45(9), 3986-3992. . https://doi.org/10.1016/j.ejmech.2010.05.054.

[19] Hayat F, Moseley E, Salahuddin A, Van Zyl RL & Azam A (2011), antiprotozoal activity of chloroquinoline based chalcones. European Journal of Medicinal Chemistry 46(5) 1897-1905. https://doi.org/10.1016/j.ejmech.2011.02.004.

[20] Shettigar S, Umesh G, Chandrasekharan K & Sarojini BK (2008), Studies on third-order nonlinear optical properties of chalcone derivatives in polymer host. Optical Materials 30(8), 1297-1303. https://doi.org/10.1016/j.optmat.2007.06.008.

[21] Asiri AM, Marwani HM, Alamry KA, Al-Amoudi MS, Khan SA & El-Daly SA (2014), Green Synthesis, Characterization, Photophysical and Electrochemical Properties of Bis-chalcones. International Journal of Electrochemical Science 9, 799-809.

[22] Shettigar S, Chandrasekharan K, Umesh G & Sarojini BK (2006), Studies on nonlinear optical parameters of bis-chalcone derivatives doped polymer. Polymer 47(10) 3565-3567. https://doi.org/10.1016/j.polymer.2006.03.062.

[23] Delavaux-Nicot B, Maynadié J & Lavabre D (2007), Ca2+ vs. Ba2+ electrochemical detection by two disubstituted ferrocenyl chalcone chemosensors. Study of the ligand–metal interactions in CH3CN. Journal of Organometallic Chemistry 692(4), 874-886. https://doi.org/10.1016/j.jorganchem.2006.10.045.

[24] Gasull EI, Blanco SE & Ferretti FH (2002), a theoretical and experimental study of adsorption from dilute cyclohexane solutions of non-electrolytes: 4-X-chalcones on silica gel. Journal of Molecular Structure: THEOCHEM 579(1-3), 121-137. https://doi.org/10.1016/S0166-1280(01)00723-0.

[25] Goto Y, Hayashi A, Kimura Y & Nakayama M (1991), Second harmonic generation and crystal growth of substituted thienyl chalcone. Journal of Crystal Growth 108(3-4), 688-698. https://doi.org/10.1016/0022-0248(91)90249-5.

[26] Frisch MJ, et al., (2009), Gaussian 09, Revision B.01, Gaussian Inc., Wallingford CT.

[27] Becke AD (1993), Density-functional thermochemistry. III. The role of exact exchange. The Journal of Chemical Physics 98(7), 5648-5652. https://doi.org/10.1063/1.464913.

[28] Lee C, Yang W & Parr RG (1988), Development of the Colle-Salvetti correlation energy formula into a functional of the electron density. Physical Review B 37 (2), 785-789. https://doi.org/10.1103/PhysRevB.37.785.

[29] Heyd J & Scuseria GE (2004), efficient hybrid density functional calculations in solids: Assessment of the Heyd–Scuseria–Ernzerhof screened Coulomb hybrid functional. The Journal of Chemical Physics 121, 1187. https://doi.org/10.1063/1.1760074.

[30] Heyd J & Scuseria G E (2004), Assessment and validation of a screened Coulomb hybrid density functional. The Journal of Chemical Physics 120, 7274. https://doi.org/10.1063/1.1668634.

[31] Frisch E, Hratchian HP, Dennington II RD, Keith TA, Millam J, Nielsen B, Holder AJ & Hiscocks J (2009), Gaussian, Inc. GaussView Version 5.0.8, Wallinford, CT.

[32] Jamroz MH (2004), Vibrational Energy Distribution Analysis: VEDA 4 Program, Warsaw, Poland.

[33] Glendening ED, Reed AE, Carpenter JE & Weinhold F (1998), NBO Version3.1, TCI, University of Wisconsin, Madison.

[34] Foster JP & Weinhold F (1980), Natural hybrid orbitals. Journal of the American Chemical Society 102(24), 7211-7218. https://doi.org/10.1021/ja00544a007.

[35] Reed AE & Weinhold F (1983), Natural bond orbital analysis of near–Hartree–Fock water dimer. The Journal of Chemical Physics 78, 4066-4073. https://doi.org/10.1063/1.445134.

[36] Reed AE & Weinhold F (1985), Natural localized molecular orbitals. The Journal of Chemical Physics 83, 1736-1740. https://doi.org/10.1063/1.449360.

[37] Reed AE, Weinstock RB & Weinhold F (1985), Natural population analysis. The Journal of Chemical Physics 83, 735–746. https://doi.org/10.1063/1.449486.

[38] Reed AE, Curtiss LA & Weinhold F (1988), Intermolecular interactions from a natural bond orbital, donor-acceptor viewpoint. Chemical Reviews 88(6), 899-926. https://doi.org/10.1021/cr00088a005.

[39] Szafran M, Komasa a & Bartoszak-Adamska E (2007), Crystal and molecular structure of 4-carboxypiperidinium chloride (4-piperidinecarboxylic acid hydrochloride). Journal of Molecular Structure 827(1-3), 101-107. https://doi.org/10.1016/j.molstruc.2006.05.012.

[40] Sebastian S & Sundaraganesan N (2010), the spectroscopic (FT-IR, FT-IR gas phase, FT-Raman and UV) and NBO analysis of 4-Hydroxypiperidine by density functional method. Spectrochimica

Acta Part A: Molecular and Biomolecular Spectroscopy 75(3), 941-952. https://doi.org/10.1016/j.saa.2009.11.030.

[41] Tamer Ö, Avcı D & Atalay Y (2015), Synthesis, X-ray structure, spectroscopic characterization and nonlinear optical properties of Nickel (II) complex with picolinate: A combined experimental and theoretical study. Journal of Molecular Structure 1098, 12-20. https://doi.org/10.1016/j.molstruc.2015.05.035.

[42] Altürk S, Tamer Ö, Avcı D & Atalay Y (2015), Synthesis, spectroscopic characterization, second and third-order nonlinear optical properties, and DFT calculations of a novel Mn(II) complex. Journal of Organometallic Chemistry 797, 110-119. https://doi.org/10.1016/j.jorganchem.2015.08.014.

[43] Stratmann RE, Scuseria GE & Frisch MJ (1998), an efficient implementation of time-dependent density-functional theory for the calculation of excitation energies of large molecules. The Journal of Chemical Physics 109, 8218-8224. https://doi.org/10.1063/1.477483.

[44] Cancès E, Mennucci B & Tomasi J (1997), a new integral equation formalism for the polarizable continuum model: Theoretical background and applications to isotropic and anisotropic dielectrics. The Journal of Chemical Physics 107, 3032-3041. https://doi.org/10.1063/1.474659.

[45] O'Boyle NM, Tenderholt AL & Langner KM (2008), cclib: a library for package-independent computational chemistry algorithms. Journal of Computational Chemistry 29(5), 839–845. https://doi.org/10.1002/jcc.20823.

[46] Ferreira MMC (1993), Population analysis from atomic polar tensors. Journal of Molecular Structure 294, 75–78. https://doi.org/10.1016/0022-2860(93)80318-P.

[47] Parr RG, Szentpály LV & Liu S (1999), Electrophilicity Index. Journal of the American Chemical Society 121(9), 1922-1924. https://doi.org/10.1021/ja983494x.

[48] Chattaraj P.K., Maiti B & Sarkar U (2003), Philicity: A Unified Treatment of Chemical Reactivity and Selectivity. Journal of Physical Chemistry a 107, 4973-4975. https://doi.org/10.1021/jp034707u.

[49] Parr RG, Donnelly RA, Levy M & Palke WE (1978), Electronegativity: the density functional viewpoint. Journal of Chemical Physics 68(8), 3801-3807. https://doi.org/10.1063/1.436185.

[50] Parr RG & Pearson RG (1983), Absolute hardness: companion parameter to absolute electronegativity. Journal of the American Chemical Society 105(26), 7512-7516. https://doi.org/10.1021/ja00364a005.

[51] Pearson RG (2005), Chemical hardness and density functional theory. Journal of Chemical Sciences 117(5), 369-377. https://doi.org/10.1007/BF02708340.

[52] Alwani Zainuri D, Arshad S, Che Khalib N, Abdul Razak I, Raveendran Pillai R, Farizaa Sulaiman S, Shafiqah Hashim N, Leong Ooi K, Armaković S, Armaković SJ, Yohannan Panicker C & Van Alsenoy C (2017), Synthesis, XRD crystal structure, spectroscopic characterization (FT-IR, 1H and 13C NMR), DFT studies, chemical reactivity and bond dissociation energy studies using molecular dynamics simulations and evaluation of antimicrobial and antioxidant activities of a novel chalcone derivative, (E)-1-(4-bromophenyl)-3-(4-iodophenyl)prop-2-en-1-one. Journal of Molecular Structure 1128, 520-533. https://doi.org/10.1016/j.molstruc.2016.09.022.

[53] Samshuddin S, Butcher RJ, Akkurt M, Narayana B, Sarojini BK & Yathirajan HS (2012), (1E,4E)-1-(3-Nitro-phen-yl)-5-phenyl-penta-1,4-dien-3-one. Acta Crystallographica Section E 68, o74-o75. https://doi.org/10.1107/S1600536811052548.

[54] Rastogi VK, Palafox MA, Tanwar RP & Mittal L (2002), 3, 5-Difluorobenzonitrile: ab initio calculations, FTIR and Raman spectra. Spectrochimica Acta Part A: Molecular and Biomolecular Spectroscopy 58(9), 1987-2004. https://doi.org/10.1016/S1386-1425(01)00650-3.

[55] Silverstein M, Basseler GC & Morill C (1981), Spectrometric Identification of Organic Compounds, Wiley, New York.

[56] Wade LG (1992), Advanced Organic Chemistry, fourth ed., Wiley, New York.

[57] Roeges NPG (1994), a Guide to the Complete Interpretation of IR Spectra of Organic Compounds, Wiley, New York.

[58] Clothup NB, Daly LH & Wiberly SE (1990), Introduction to IR and Raman Spectroscopy, Academic Press, New York.

[59] Socrates G (1981), Infrared Characteristic Group Frequencies, John Wiley and Sons, New York.

[60] Meislich EK, Meislich H & Sharefkin J (1993), 3000 Solved Problems in Organic Chemistry, vol. 2, McGraw–Hill, New York.